Pergamon

Journal of Structural Geology, Vol. 18, No. 12, pp. 1399 to 1415, 1996

PII: S0191-8141(96)00066-1
0191-8141/96 $15.00 + 0.00

Flexural-slip generated bedding-parallel veins from central Victoria, Australia

T. J. FOWLER

Geology Department, La Trobe University Bendigo, P.O. Box 199, Bendigo, Victoria 3550, Australia

(*Received* 8 *March* 1996; *accepted in revised form* 24 *July* 1996)

Abstract—Thin continuous laminated bedding-parallel quartz veins (BPVs) with slip-striated and fibred vein walls occur within slates, or at their contact with sandstones, on the limbs of chevron folds in the Bendigo–Castlemaine goldfields, southeastern Australia. Two microstructural Types of BPV (I and II) have been previously recognized, and are confirmed in this study. Both types are concluded to have formed during and/or after crenulation cleavage (the first tectonic axial planar structure) in the wallrock slates, and during flexural-slip folding. Type I BPVs consist of syntaxial phyllosilicate inclusion trails, parallel to bedding, enclosing inclined inclusion bands, the latter formed by detachment of wallrock phyllosilicate particles from the walls of pressure solution-segmented discordant tension veins. Type I BPVs are formed by bedding-parallel shear, and grow in width by propagation of the discordant veins into the BPV walls. Type II veins are composed of quartz bands separated by wallrock slate seams which have split away from the vein wall during dilatant shear opening. They incorporate numerous torn-apart fragments of crenulated wallrock slate. Type I BPV inclusion band average spacing of 0.5 mm probably represents the magnitude of slip increments during stick-slip flexural-slip folding activity. Copyright © 1996 Elsevier Science Ltd

INTRODUCTION

Bedding-parallel, typically laminated quartz veins (BPVs) are most frequently reported from chevron-folded low-grade metamorphosed turbidite successions around the world (Tanner 1989). These veins are generally thin (mms to tens of cms thick) but are typically continuous for tens to several hundreds of metres along their dip and strike directions, and are reported to be spatially associated with the fold structures. Many of the veins bear slip lineations and fibre lineations on their walls (and on the laminations within the veins) which have been attributed to shear-opening of the veins before or during folding. The following is a summary of the pre-folding, early-folding and syn-folding models which have been proposed for the origin of BPVs.

Pre-folding model

The BPVs result from syn-sedimentary submarine hydrothermal exhalations (Haynes 1987) or, more popularly, basinal fluid overpressures which have hydraulically jacked apart near-horizontal bedding planes (Figs. 1a & b) (Nicholson 1978, Boulter 1979, Graves & Zentilli 1982, Stoneley 1983, Fitches *et al.* 1986, Henderson *et al.* 1990, Cosgrove 1993 (in part)). The fluid overpressures may result from evolution and thermal expansion of fluids during burial or by expulsion of pore fluids during compaction, with fluid escape being inhibited by reduction of sediment permeability, for example, by cementation. The close association of the veins with folds has been explained in terms of pre-tectonic doming of sedimentary layers by pooling of fluids beneath them, with localization of later anticlines in these zones of low bedding cohesion (Price & Cosgrove 1990). Shear-opening of veins is interpreted to reflect either gliding of detached sediment slices down basin slopes, or perhaps thrusting preceding folding (Cosgrove 1993). The evidence for a pre-folding origin of BPVs includes: (i) common folding of veins and their overprinting by cleavages (Fitches *et al.* 1986); (ii) tabular vein minerals

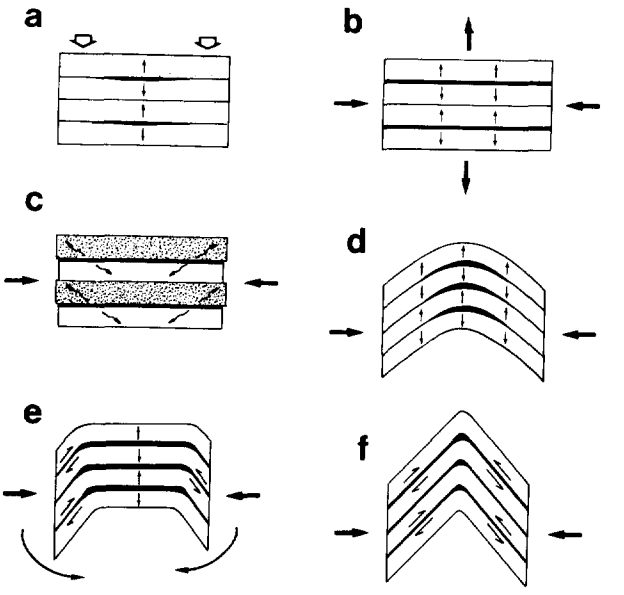

Fig. 1. A sketch of models proposed to explain the origin of bedding-parallel veins which are commonly associated with folded turbidites. (a) 'Hydraulic jacking' apart of beds due to basin fluid overpressures during sedimentary compaction (Fitches *et al.* 1986, Henderson *et al.* 1990). (b) A variant of (a) where hydraulic jacking is effected by early tectonic compression (or shearing) parallel to beds, and rapid evolution of fluids by metamorphism (may be pre- or post-cleavage in the timing of vein development) (Graves & Zentilli 1982). (c) Buttressing by competent sandstones in the earliest stages of folding, while incompetent siltstones continue to shorten homogeneously, leading to detachment along bedding planes with the reverse sense of shear opening to that of later flexural-slip folding (Jessell *et al.* 1994). (d) 'Compatible folding' where axial plane-parallel extension occurs during folding whilst bed thickness is kept constant (Smith & Marshall 1993). (e) A variant on the dilatant kink band model (Ramsay 1967) adapted to boxfolds where dilation along the median segment is due to steepening of boxfold limbs (with or without boxfold hinge migration) (Fowler & Winsor 1996). (f) Flexural-slip folding origin by dilatant shearing along movement horizons (Tanner 1989, Cosgrove 1993 (in part)).

bent around fold hinges (Nicholson 1978); (iii) veinwall-normal quartz columns and fibres (Henderson *et al.* 1986, Henderson *et al.* 1990, Cosgrove 1993); (iv) extreme variability in slip striation or slip fibre orientations within single veins (Fitches *et al.* 1986); (v) constant vein-opening shear sense indicators, across fold hinges; and (vi) the continuity of BPVs across fold hinges with no evident changes in vein thickness associated with hinge zones (Cosgrove 1993,1995).

Early-folding model

The BPVs have formed after the onset of folding but before limb dips of several degrees have been attained (Boulter 1979, Jessell *et al.* 1994, Cosgrove 1995). The vein-opening mechanism is again hydraulic jacking by basinal fluid or early metamorphic fluid overpressures. Differential layer shortening of competent and incompetent beds during the earliest stages of folding (Fig. 1c, Jessell *et al.* 1994) has been proposed to explain the reversal across fold hinges of the shear sense associated with BPV growth, where these shear senses were opposite to those expected for flexural-slip folding. BPVs are overprinted by later folding events (flexural-slip activity, late fold nucleation, fold-flattening and cleavage formation). Evidence for an early-folding origin of BPVs includes: (i) BPVs being folded and overprinted by a 'stripey' cleavage (which is demonstrated to have formed before several degrees of limb dip) (Boulter 1979); and (ii) reversals of BPV shear sense indicators across hinges, but opposite to that expected for flexural-slip folding (Jessell *et al.* 1994).

Syn-folding model

The BPVs develop during folding as a result of metamorphic fluids being drawn into dilating slip-horizons or hinge zones during flexural-slip folding, with pumping or trapping and channelling of fluids along dilating anticlinal or domal hinge zones (Figs. 1d–f) (Barnett & Chamberlain 1988). The resulting abnormal fluid pressures are thought to promote hydraulic fracturing (Keppie 1976, Boyle 1986, Mawer 1987, Tanner 1989, Cosgrove 1993 (in part)). Other interpretations in which bedding-parallel voids occur in broad hinge zones (rather than along flexural-slip active planes), as limb-dip accommodating mechanisms are shown in Fig. 1(d) and (e) and are discussed in Smith & Marshall (1993) and Fowler & Winsor (1996). Evidence for a syn-folding origin of BPVs includes: (i) consistent near-orthogonality between local fold hinges and the average of slip-lineation orientations on veinwalls (Tanner 1989,1990); (ii) reversal of vein opening shear-sense indicators across fold hinges (Tanner 1989,1990); (iii) correlation between fold style parameters (e.g. fold curvature, shape, inter-limb angle) and spacing, geometry and occurrence of BPVs (Keppie 1976, Mawer 1987, Tanner 1989); (iv) BPVs which truncate wallrock axial planar cleavage or incorporate slices of it, and show weak or no deformation (Mawer 1987,1989); (v) corresponding slip-lineations on veins on opposite fold limbs not unfolding to a single orientation (Tanner 1989); (vi) correlation between BPV vein thickness and flexural slip displacement of sedimentary dykes (Tanner 1989); and (vii) the tendency for BPVs to become indistinct towards hinges and the inability to correlate many of these veins across fold hinges (Tanner 1989).

There are strong differences of opinion regarding the relevant model for BPV formation even amongst studies from the same region. Thus Mawer 1987, 1989 proposed a late syn-folding origin for BPVs from the Meguma Group, Nova Scotia, and was challenged by Henderson *et al.* (1989) who supported a pre-folding BPV origin for the same veins. Tanner 1989, 1990 argued for a syn-folding origin of BPVs from the Welsh Basin, which was challenged by the pre-folding model of Fitches *et al.* (1990) for veins from the same basin. The controversy surrounding pre- versus syn-folding BPVs reflects similar problems in other pre-versus syn-deformational geological events, from granite intrusions to porphyroblast growth: pre- and syn-folding BPVs share many common features, and continuing deformation may destroy much of the earlier evidence. Pre- and syn-folding models may not be mutually exclusive, for example Tanner (1990) tentatively noted the possibility that pre-folding BPVs could form during layer-parallel shortening and control the subsequent location of slip surfaces in later folding, and Henderson *et al.* (1990) also consider the continuous evolution of pre-folding BPVs into the stage of fold development.

This paper describes the BPV microstructures of veins from a region of chevron-folded turbidites in central Victoria, Australia, specifically the Bendigo and Castlemaine goldfields. Evidence is presented which indicates that the majority of these veins are approximately synchronous with (or postdate) the development of the crenulation cleavage (which is a first generation tectonic structure, axial planar to the chevron folds) in the slate vein walls, and that BPV microstructures are consistent with a flexural-slip folding origin.

Structural setting of the Bendigo–Castlemaine goldfields

The Bendigo–Castlemaine goldfields lie in the Ballarat Slate Belt of central Victoria, Australia. In this region the 2000+ m thick Lower Ordovician quartz-rich turbiditic sandstones and siltstones (now metasandstones and slates) have been deformed during the mid-Devonian Tabberabberan Orogeny into upright to steeply inclined NNW-trending folds, with hinges gently to moderately plunging to the north and south. Folds are continuous for tens of kilometres along strike and down axial planes, and have wavelengths of 200–300 m (Stone 1937, Thomas 1953, Gray 1988, Ramsay & Willman 1988, Cox *et al.* 1991, Gray & Willman 1991, Willman & Wilkinson 1992).

In the sandstones a convergent fanning spaced 'stripey' solution cleavage is well-developed in the inner arcs of fold hinge zones, and formed before 15° fold limb dips were exceeded (Yang & Gray 1994). This stripey cleavage

is overprinted by an axial planar grain alignment cleavage, associated with fold flattening during the same deformation event (Yang & Gray 1994). The axial planar structure in the slates is a crenulation cleavage which overprints a bedding-parallel mica fabric, the latter perhaps related to earlier sedimentary compaction (White & Johnston 1981). The crenulation cleavage then is the *first* tectonic foliation imposed on these rocks. Details of the microstructure of the crenulations are described later.

The folds have an approximate chevron style but there are notable deviations from chevron fold geometry for some layers (Fowler & Winsor in press). Fold interlimb angles are typically 40° or less. The folded sequence is divided into tectonic slices tens of km wide, bound by westerly-dipping thrust faults. Studies of fold interlimb angles and porphyroblast pressure shadow geometries indicate increasing shear strain towards the boundary thrusts, suggesting thrusting and folding were contemporary processes at some stage (Gray & Willman 1991).

Outcrop characteristics of BPVs

In the Bendigo–Castlemaine goldfields, BPVs are located almost exclusively in slate beds, particularly within 10 cm of an overlying sandstone bed. BPVs are not uniformly spaced in a stratigraphic sense. On the basis of detailed underground surveys of the mines in the goldfields, an average BPV stratigraphic spacing of 13 m was reported by Jessell *et al.* (1994), and typical vein thicknesses ranging from 50 to 200 mm were noted. However, measurements of continuous exposures in railway cuttings in the same region indicate BPV average spacing of 9 m, and average vein thickness <20 mm (Fowler & Winsor, unpubl. data), suggesting that most of the thinner BPVs were consistently overlooked in the mine surveys. Thickness variations along strike are gradual and Jessell *et al.* (1994) noted BPVs defined by a ring of gently tapering quartz lenses. Some BPVs show gradual thickness increases towards anticlinal fold hinges.

The mine sections described above demonstrate that BPVs thicker than about 50 mm are commonly traceable as continuous vein structures across macroscopic fold hinges, whereas BPVs thinner than 10 mm (representing about 50% of the BPV population) are typically not correlatable across fold hinges. Where BPVs are present at fold hinges these veins are often tightly folded and overprinted by axial planar pressure solution cleavage stripes. Folding of BPVs and slip striations on the limbs of folds are also locally observed (Jessell *et al.* 1994). Later limb thrusts are locally found in association with thick BPVs (Willman 1988), which are commonly referred to as 'backs' or 'leg reefs'.

Lineations on BPV walls are defined by slickenside slip-striations, and quartz fibres and fibre casts. The average orientation of these lineations is orthogonal to the local fold axis, although deviations up to 60° from this orientation are developed in some examples even within a single vein.

BPVs are commonly associated with and may pass into bedding-discordant quartz veins called 'spurs' which are filled with coarsely crystalline, fibrous or vuggy quartz. The spurs are strongly tapering and gash-like tensional veins which form parallel stacked arrays particularly in the stronger sandstone beds. Some spurs, especially those in slates, are folded and overprinted by cleavages.

BPV terms and microstructural types

Oriented samples of BPVs were collected from the limbs of the Derby, Garden Gully, New Chum and Apollo anticlines in Bendigo, and an unnamed anticline lying 1 km east of Castlemaine. All descriptions and figures of vein microstructures presented here pertain to thin sections cut normal to the vein and parallel to the dominant slip lineation on the vein walls, and observed looking north, unless stated otherwise. Terms used to describe the microstructural features of BPVs are shown in Fig. 2. Note that the terms inclusion 'band' (Fig. 2a) and inclusion 'trail' (Fig. 2b) refer to distinct microstructures (Ramsay 1980, Cox 1987). Inclusion 'bands' refer to subparallel lines of minute solid inclusions which reflect the detailed topography of the veinwall from which they have been plucked, with all the members of a single band detaching from the vein wall approximately simultaneously during a single crack–seal vein opening increment. An inclusion 'trail' is also a linear trace of an inclusion surface, however each particle in the trail is plucked during consecutive crack–seal increments. The trail traces out the displacement path related to the opening of the vein.

Microstructural studies of BPVs of the Bendigo–Castlemaine area have been reported previously by Jessell *et al.* (1994). A detailed description of Jessell *et al.*'s model for BPV formation is presented later, so as to avoid repetition when comparing their model with the one supported in this study. Willman (1988) and Jessell *et al.* (1994) discovered two characteristic BPV microstructural types (Types I and II) from Bendigo–Castlemaine region, which are confirmed in this study. Type I BPVs (Figs. 2a & 3a–c) are rarer (<10% of BPVs), thinner (typically <20 mm), and consist of thin laminae (averaging 0.25–0.5 mm thickness) of vein quartz separated by thin (10 microns thick) layer silicate and carbonate inclusion trails which lie within a degree or two of parallelism to the veinwalls. Pairs of inclusion trails enclose phyllosilicate inclusion bands which lie systematically inclined to the vein walls (Fig. 3a). Jessell *et al.* (1994) devised the term 'inclusion surface trace' (IST) to cover both the low angle inclusion trails and higher angle inclusion bands. Because of the need to clearly distinguish the inclusion trails from the inclusion bands, the term IST is not used in this study, except in the discussion of their model.

Type II BPVs (Figs. 2b & 3d) are thicker (up to several 100s mm), and consist of millimetre to centimetre thick bands of (sometimes vuggy) quartz. The term 'quartz band' is used for Type II veins, while 'quartz laminae' is used for Type I veins, since these two sheeted structures

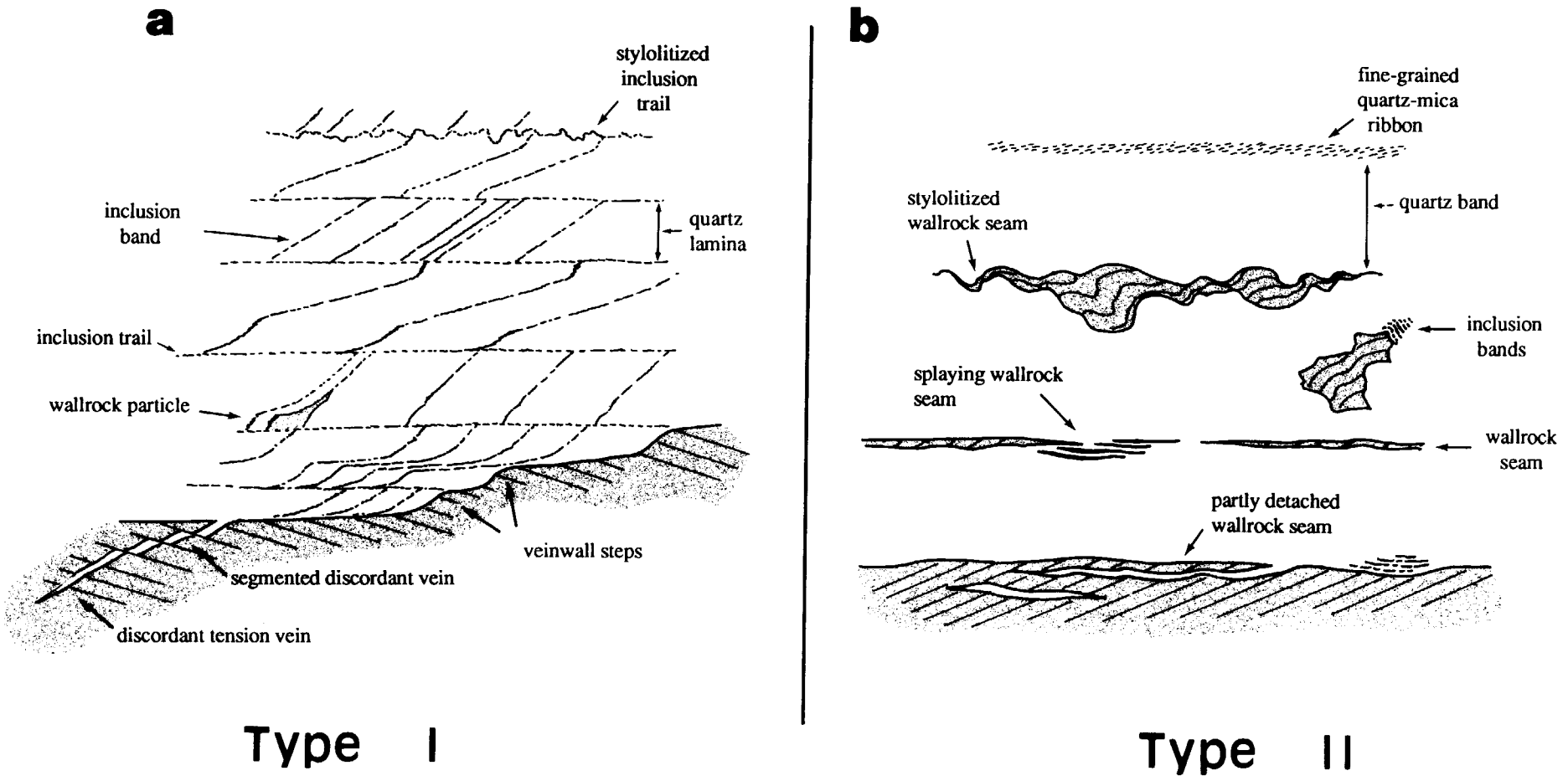

Fig. 2. Sketch of the typical microstructural features of Type I and Type II BPVs, and the terms used to describe them in this paper. Crenulation cleavage orientation is represented by oblique lines in the veinwalls. (a) Type I veins. (b) Type II veins.

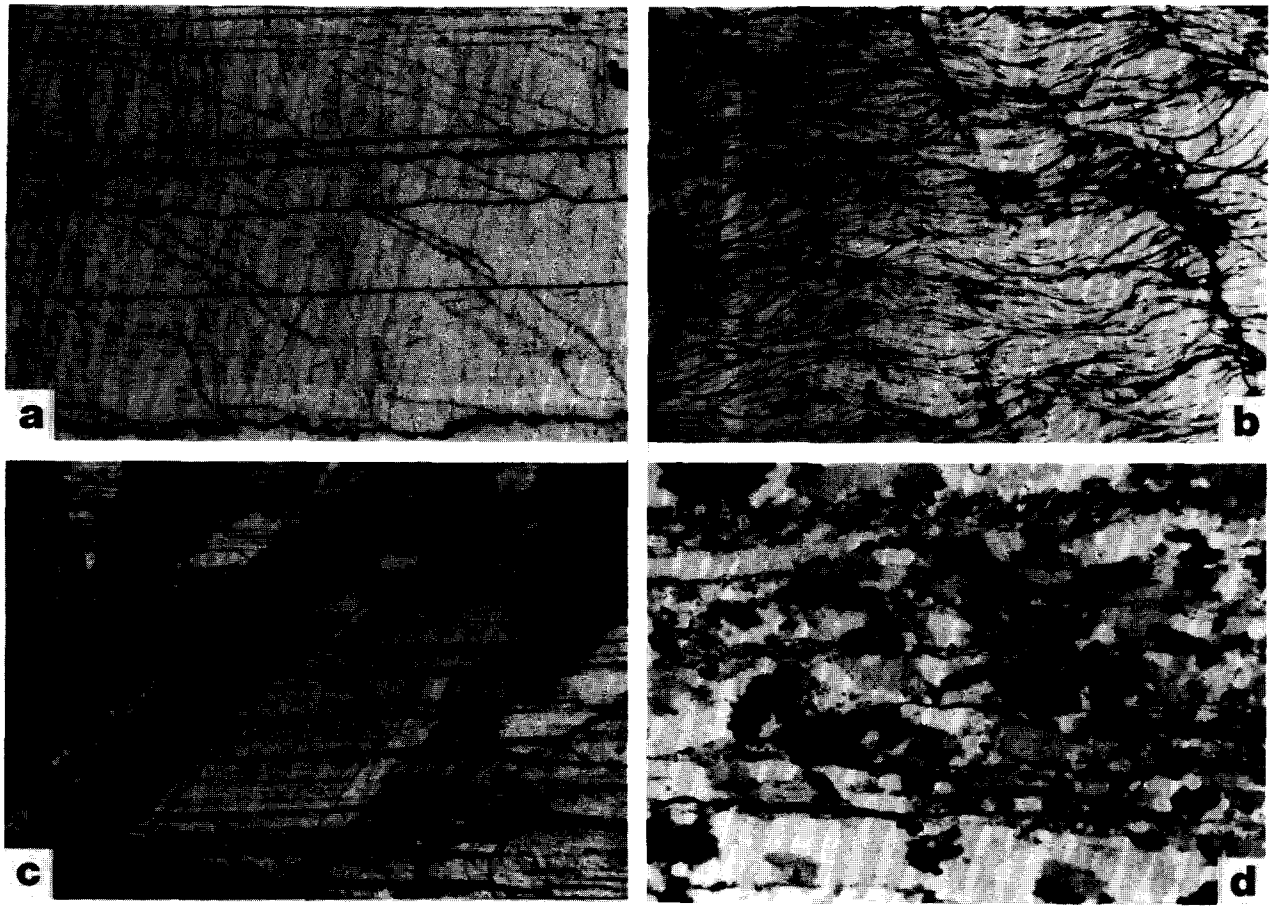

Fig. 3. Examples of BPV Type I and Type II microstructures from the Bendigo–Castlemaine goldfields. (a) Type I BPV showing inclusion trails (parallel to the long edge of the photograph), with inclusion bands between them showing a consistent sense of inclination to the inclusion trails. Note the stepped inclusion bands and the stylolitized inclusion trail in the lowest lamina (from the west limb of the New Chum Anticline, Victoria Hill). (b) Type I BPV showing the undulating traces of inclusion trails and bands in a section cut normal to the slip lineation (from the east limb of the Derby Anticline, Eaglehawk). (c) Type I BPV showing quartz columns extending across inclusion trails and showing a consistent sense of inclination (from the western limb of the Garden Gully Anticline, Eaglehawk). (d) Type II BPV with wallrock seams parallel to the long edge of the photograph (from the west limb of the Apollo Hill Anticline, White Hills). In (a) to (d) the length of the long edge of the photographs is 2.2 mm.

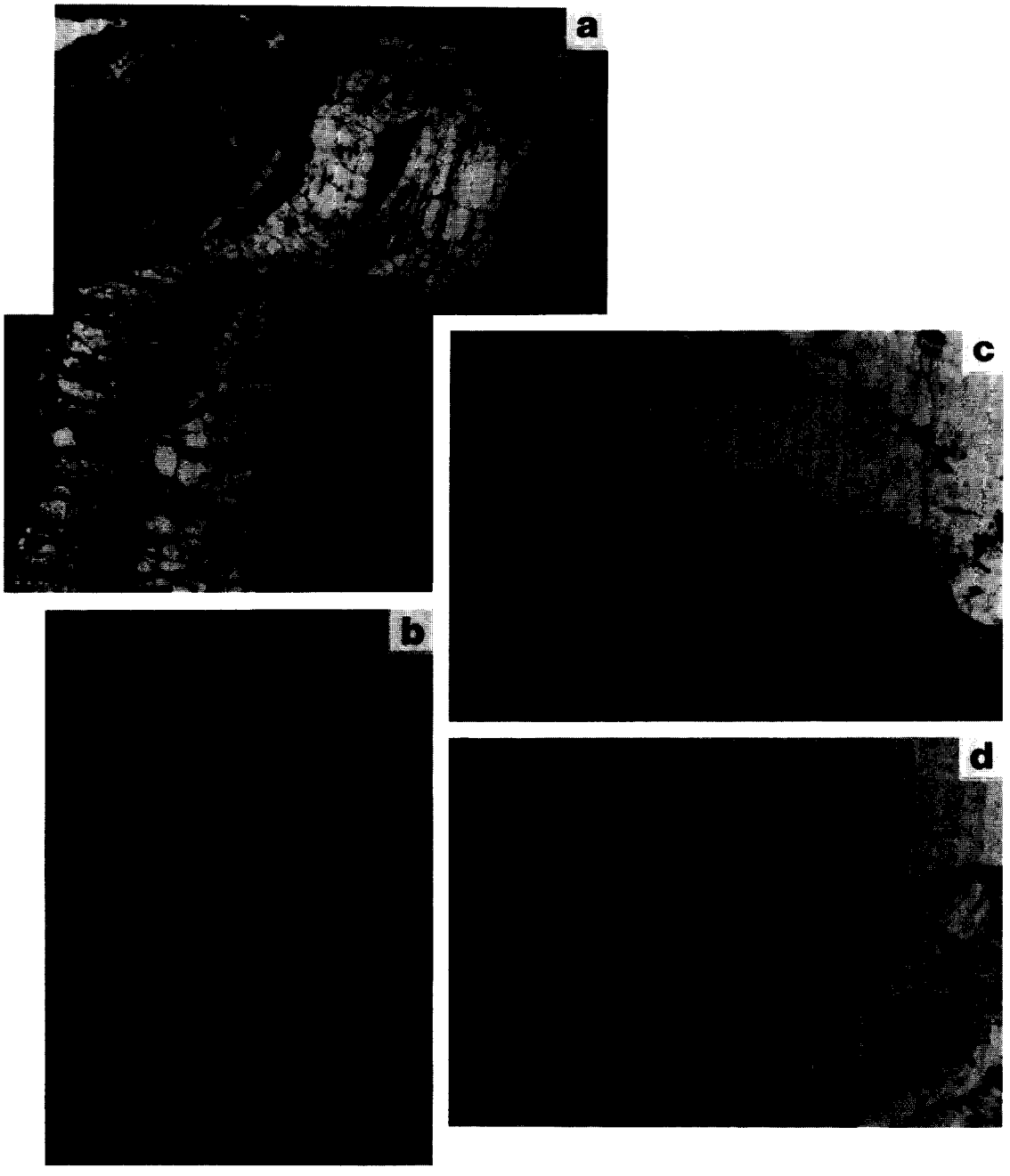

Fig. 4. Microstructural features of BPV walls. (a) Rhomb-opening of tension veins in veinwall. A transform structure separates the upper tension vein from the lower. Wallrock inclusion bands are developed parallel to the vein walls. Opening direction lies parallel to the transform (from the western limb of the New Chum Anticline, Victoria Hill). (b) Inclusion bands developed along the upper edge of a discordant tension vein. Vein opening direction was approximately parallel to the crenulation cleavage in the vein wall (from the western limb of the Apollo Anticline, White Hills). (c) Two small imbricate thrust structures (dipping gently to the right) at the vein wall contact (from the eastern limb of the Derby Anticline, Eaglehawk). (d) Tension gashes in the veinwall (eastern limb of the Derby Anticline, Eaglehawk). The length of the long edge of the micrographs is as follows: (a) 2.2 mm (along the top edge). (b) 0.83 mm, (c)–(d) 2.2 mm.

Fig. 5. Micrographs of critical characteristics of Type I BPV inclusion bands (see text for discussion). (a) Crenulated wallrock slate fragments detached during vein growth. Note the conformity of the shape of inclusion bands to the changing shape of the fracture edges of the fragments. (b) Detail of the left hand wallrock fragment in (a) showing the crenulation cleavage in the fragment, and micas defining the inclusion bands parallel to its fracture edge. (c) Crenulated wallrock sliver detached during inclusion band formation. Note the conformable shape of the inclusion band to its left. (d) Segmented discordant vein with inclusion bands parallel to the vein walls. The segments are separated by prominent crenulation cleavage stripes which are traceable into inclusion trails (for example, the surface which approximately bisects the photograph lengthwise). (e) Detail of the inclusion bands in two of the vein segments in (d). (f) Typical lumpy, knotted fabric of micas defining an inclusion band. (a)–(e) are from the eastern limb of the Deborah Anticline, Bendigo, (f) is from the western limb of the New Chum Anticline, Victoria Hill. The length of the long edge of the micrographs is as follows: (a) 4.52 mm, (b)–(c) 0.82 mm, (d) 2.2 mm, (e) 0.87 mm, (f) 0.52 mm.

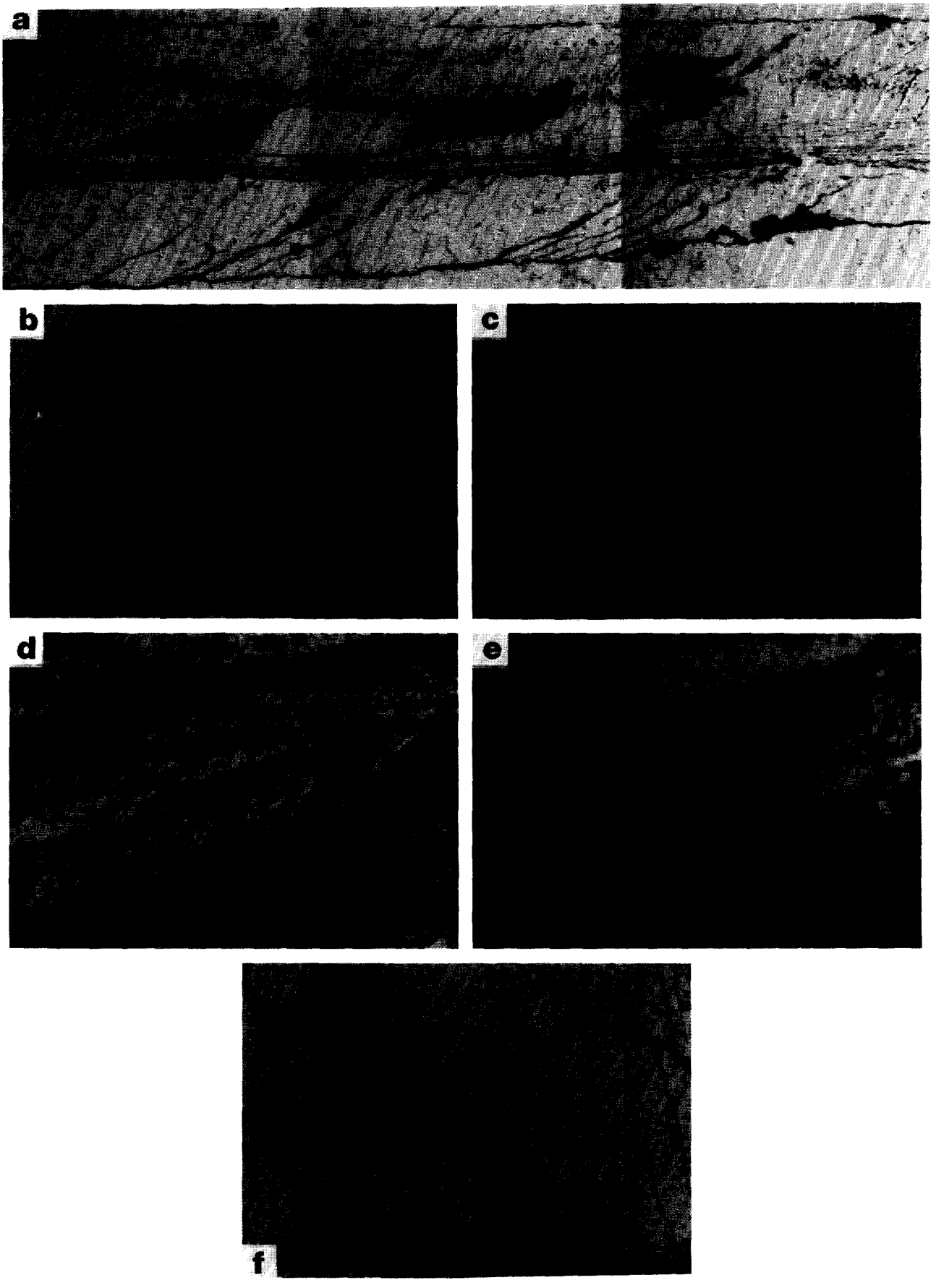

Fig. 5

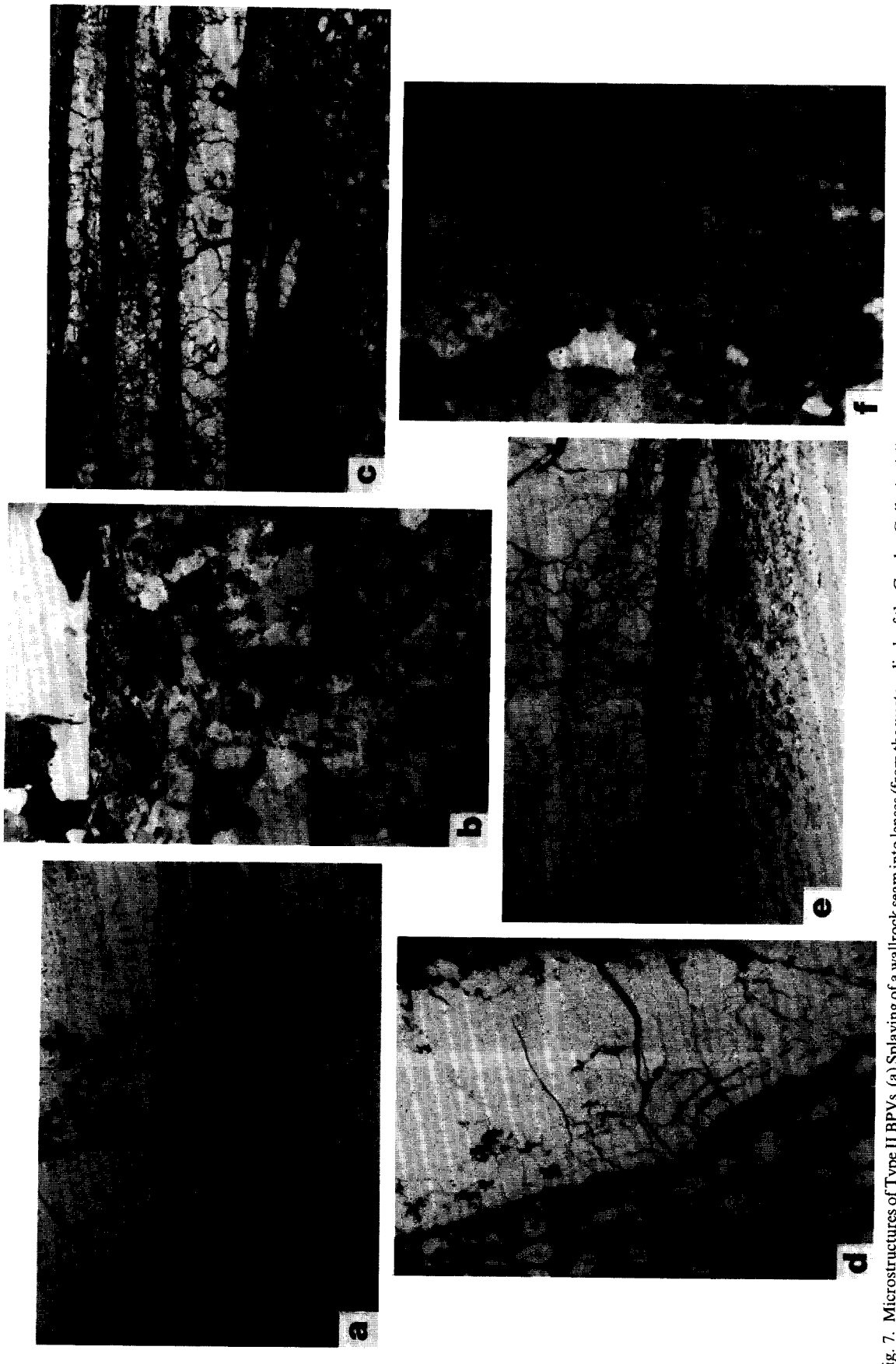

Fig. 7. Microstructures of Type II BPVs. (a) Splaying of a wallrock seam into lenses (from the western limb of the Garden Gully Anticline, Eaglehawk). (b) Bands of vein quartz (partly crossed polars) with scattered fragments of crenulated wall rock slate (from the western limb of unnamed anticline one kilometre east of Castlemaine). (c) Vein-wall contact showing tensional veins nearly parallel to the vein wall (same location as for (c)). (d) Inclusion bands with their shape dictated by vein wall irregularities (from the eastern limb of the Derby Anticline, Eaglehawk). (e) Detached wallrock seam near vein wall (from the western limb of the Garden Gully Anticline, Eaglehawk). (f) Ribbon of fine-grained quartz (greys) and displacement-oriented mica (white particles). Mica (001) planes are oriented at a low angle to the length of the ribbon and dip steeply to the left (from the eastern limb of the Derby Anticline, Eaglehawk). Length of the long edge of the micrographs is as follows: (a) 0.82 mm. (b)–(e) 2.2 mm. (f) 0.86 mm.

have quite different origins, as explained below. The quartz bands are separated by discontinuous lumpy seams of wallrock slate ('ribbon' structure of Chace 1949 and McKinstry & Ohle 1949), which are approximately parallel with the veinwalls. Only traces of inclusion bands are developed, as described below. Some examples of Type II veins are intensely deformed, folded and stylolitized, while (identifiable) Type I veins show only weak deformation.

Type I and II veins are not distinguished by their structural settings. Indeed it is possible to sample Type I and Type II veins from the same laminated vein, and they are found as composite veins in thin section. Details of the microstructure of BPV Types I and II are given below, following a brief description of the microstructure of the slate wallrocks.

BPV WALLROCK MICROSTRUCTURES

Most BPVs (of either type) have hangingwalls and footwalls of slate, showing a closely-spaced, axial-planar, crenulation cleavage which lies between 13° and 36° (averaging 24°) to the vein wall. The cleavage-to-vein angle may change within a millimetre of the vein wall, giving gently curved cleavage traces. In most cases this 'drag' flexure is consistent with the shear sense expected on the vein due to flexural-slip folding. Where the latter flexure is not consistent with flexural-slip sense of shear, there is evidence of extension parallel to the vein leading to increase in the angle between the cleavage and veinwall. Localised asymmetric microfolds in the cleavage traces and small-scale imbricate thrusts of slices of wallrock slate (two of the latter are shown in Fig. 4c) are found at Type II (but not Type I) vein contacts, with a sense consistent with the shear associated with flexural-slip folding. Minor kinking and later generation rare crenulations are developed nearest the vein walls. All of the above structural features may be seen in BPV footwalls and hangingwalls.

The crenulation cleavage microstructures of slates in this region have been described by White & Johnston (1981) and Stephens *et al.* (1979). The crenulation cleavage is defined by continuous anastomosing mica and chlorite-rich *P*-domains (typically 0.015 mm wide) representing former limbs of crenulation microfolds. The phyllosilicate (001) planes lie either parallel to the domain or are inclined up to 10° to the length of the domain such that the (001) planes always lie in the acute angle defined by cleavage and bedding. The *P*-domains alternate with quartz-richer *Q*-domains (typically 0.025 mm wide), the latter representing modified crenulation microfold hinges. Mica and chlorite flakes in *Q*-domains are coarser-grained and have (001) planes disposed at large angles to the domain boundaries. The crenulation cleavage overprints an earlier bedding-parallel phyllosilicate fabric (White & Johnston 1981) which may have been formed during sedimentary compaction.

BPV wall marginal veins

Near Type I and II BPV contacts it is common to find examples of marginal veins. Most commonly these are crenulation cleavage-discordant veins extending a few millimetres into either vein footwall or hangingwall margins (Figs. 4b & d and 5d & e) and lie at angles between 42° and 116° to the BPV wall (measured in the opposite sense to bedding–cleavage acute angles on fold limbs).

In Type I BPVs, angles higher than 50° between discordant vein and BPV are rare. The discordant veins are tabular or taper away from the BPV, and may show microfolding by the wallrock crenulation cleavage, or may be divided into segments by prominent *P*-domains (cleavage stripes) (Figs. 5d & e). In the latter case it appears that pressure-solution effects associated with crenulation cleavage development (Gray 1979) have overprinted these veins. Discordant vein segments show offsets with opposite sense to that expected for the shear operating along the BPV during flexural-slip folding (Fig. 5d). The sense of offset of the vein segments is consistent with their formation by pressure solution removal of vein quartz during development of crenulation cleavage stripes.

In Type II BPVs, the discordant veins typically lie at 70° or more to the BPV and appear most commonly associated with extension of the veinwalls and boudinage of the veins parallel to their length. These discordant veins are not often deformed and may be related to late stage limb stretching.

Discordant veins in both Type I and II BPVs may show sets of inclusion bands parallel to the discordant vein edge (Figs. 4a & b and 5e) suggestive of a crack–seal vein opening mechanism. Vein opening directions lie at a large angle to the discordant vein wall (Figs. 4a & d), and in Type I veins lie parallel to the inclusion trails as discussed below. The discordant veins in both types of BPV may assume rhombic form (Figs. 4a & 5d) as a result of opening of tabular veins or vein segments between 'transform' (that is, shear band) or shear structures similar to those described by Gaviglio (1986) and Labaume *et al.* (1991). Lensoidal veins approximately parallel with or lying at a low angle to BPV walls are also notable in Type II veins (Fig. 7c).

Type I bedding-parallel veins

Inclusion trails. The most characteristic feature of Type I veins are the veinwall-parallel inclusion trails separating quartz laminae and enclosing inclined inclusion bands (Fig. 3a). On careful inspection, what appear to be sets of very close-spaced inclusion trails are usually seen to be the long parallel 'flats' of low-angle stepped inclusion trails with the 'risers' being represented by inclined inclusion bands (see the inclusion trails and bands nearest the vein wall in Fig. 2a). The inclusion trails are defined by minute mica, chlorite and opaque particles. The phyllosilicate (001) planes in the trails may lie either parallel to the trail (as noted by Jessell *et al.* 1994) or

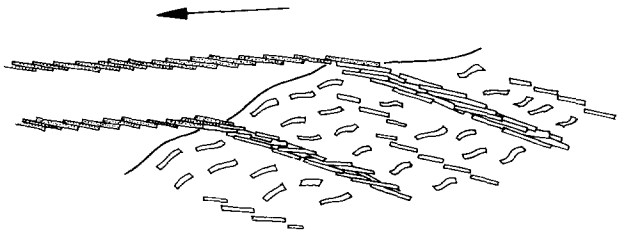

Fig. 6. A sketch explaining the different *en échelon* sense of obliquity of mica (001) planes in the inclusion trails of Type I BPVs compared to the mica (001)s in the veinwall slate *P*-domains. In the wallrock crenulation cleavage *P*-domains the mica (001) planes lie at a low angle to the domain boundary but show overall a right-handed *en échelon* sense. The mica (001) planes in the inclusion trails have a left-handed *en échelon* sense. The change in sense of mica (001) plane obliquity is due to the direction of opening of the vein (shown by the arrow) lying more counterclockwise to the *P*-domain than the orientation of the *P*-domain mica (001) planes.

inclined to it by a few degrees, forming an *en échelon* pattern. The sense of inclination is consistent along the trail and throughout the vein. If the veins were unfolded, the *en échelon* phyllosilicate (001) planes would dip gently away from the anticlinal hinges.

Inclusion trails are usually traceable back to a cleavage stripe (a prominent continuous *P*-domain) in the wallrock slate. The *en échelon* sense of obliquity of phyllosilicate (001)s in the inclusion trail is always *opposite* to that shown by phyllosilicate (001)s in the cleavage stripe (Fig. 6). The wallrock cleavage *P*-domains in Fig. 6 show mica (001) planes lying at a low angle to the domain boundary but showing overall a right-handed *en échelon* sense. The mica (001) planes in the inclusion trails have a left-handed *en échelon* sense. The change in sense of mica (001) plane obliquity is due to the direction of opening of the vein (shown by the arrow in Fig. 6) lying more counterclockwise to the *P*-domain than the orientation of the *P*-domain mica (001) planes. The opposite sense of *en échelon* obliquity demonstrates that these inclusion trails are not particles plucked from the wallrock cleavages but must be syntaxially overgrown micas detached during crack–seal vein growth as described by Ramsay (1980), Ramsay & Huber (1983), Cox & Etheridge (1983) and Cox (1987). These trails therefore track the opening direction of the Type I veins, which lies parallel to the vein walls.

Inclusion bands

The inclusion bands are usually continuous across a lamina and have constant dip sense such that if the BPVs were unfolded, the bands would always dip towards the anticlinal hinges. The angle between inclusion bands and the veinwall varies from a few degrees to 90°, but is typically 20–25° (in agreement with Jessell *et al.* 1994). Steeper bands are usually associated with thicker laminae, and low-angle bands with narrow laminae. This average inclination is lower than the common range of 50–60° reported by Labaume *et al.* (1991) for their inclusion bands. The inclusion bands typically have a stepped or gently curved appearance and the angle between them and the boundary inclusion trails may decrease gradually or remain constant as the boundaries of a lamina are neared. In this manner they differ from the inclusion bands described by Gaviglio (1986) where the inclusion bands always subtended a large angle with the boundary shear plane 'below' and a lower angle against boundary shear 'above'. The inclusion bands in a single quartz lamina generally have the same shape, although there are systematic departures from this arrangement, as described below.

The layer silicate flakes defining the inclusion bands form strings or tiny clumps of mica and chlorite flakes which have (001) planes in variable orientations, some having a ropy or microfold appearance (Fig. 5f). The thickness of the inclusion bands varies from 10 to 50 μm even along a single band. The bands are spaced (parallel to the vein wall) about 0.15–0.6 mm (typically 0.5 mm). The average spacing shows no relationship to the width of the lamina and varies only slightly amongst the laminae from the same vein. The common spacing for inclusion bands reported by Cox & Etheridge (1983), van der Pluijm (1984), Gaviglio (1986), Labaume *et al.* (1991) and others is 5–50 μm, that is, significantly smaller than those reported here. Unlike the inclusion bands described by Cox & Etheridge (1983) and Cox (1987), the phyllosilicate (001) planes do not have constant orientation within a band (Figs. 5b & f) and there are usually no inclusion trails passing through the inclusion bands.

Wallrock crenulated slate particles may be seen to adhere to some of the inclusion bands and (less commonly) to the inclusion trails (Figs. 5a & c). Some of these wallrock particles have become fragmented with the extension direction lying approximately parallel to the veinwall (Fig. 5a). From these examples, it is also clear that the inclusion bands are parallel to the fractured edges of these wallrock particles (Figs. 5a–c) and have formed either by plucking of layer silicates from the fracture edges during antitaxial crack–seal vein opening, or by detachment of syntaxially overgrown micas from the fracture edge, or both. Successive inclusion bands in a single quartz lamina show shape modifications in concert with the changing shape details of the fracture surfaces of the wallrock particles as fragmentation proceeded, as described by Labaume *et al.* (1991) (Fig. 5a). Some inclusion bands are thick enough to show the crenulation morphology of the wallrock parent (Fig. 5c), and these may be traced into wallrock fragments which are attached to the inclusion trails.

Where vein walls are present, the inclusion bands are seen to be parallel to the risers of step-like irregularities in the veinwall as illustrated by Cox (1987). These risers are themselves parallel to the walls of segmented discordant quartz veins (Fig. 5d).

The inclusion trails may show stylolitization, though this is rare in the inclusion bands. In sections normal to the slip lineation, both inclusion trails and bands are represented by an anastomosing pattern (Fig. 3b) (Jessell *et al.* 1994).

On the basis of the above microstructures it is clear that the path of vein opening for Type I veins lies parallel to the inclusion trails hence lies parallel to the bedding. Also the phyllosilicate inclusion trails are developed upon crenulation cleavage stripes in the wallrock slate, hence the timing of Type I vein growth must be either during or after crenulation cleavage development in the host slates. These conclusions differ from the pre-folding interpretation by Jessell *et al.* (1994) of BPV microstructures from this region, and are discussed below.

Type I BPV quartz microstructures

Quartz grains in Type I veins are dominantly coarse to very coarse-grained (commonly tens of mm long). Individually these grains are optically continuous across many laminae, and may be anhedral, though they are commonly elongate, forming columns with long axes inclined (25°–60°) to the inclusion trails. The sense of inclination of the quartz columns is always opposite to that of the inclusion bands (Jessell *et al.* 1994), and the angle of inclination does not vary greatly along the laminae (Fig. 3c). The quartz columns show weak to very strong undulose extinction, deformation lamellae and the development of subgrains. Extinction domains may coincide with stylolitized inclusion trails. Some laminae are partly composed of much finer-grained quartz, and their grainsize is noticeably finer adjacent to some inclusion trails, perhaps due to the growth inhibiting effects of finely dispersed mica flakes near the trails. No consistent direction of competitive grain growth was obvious in these BPVs.

Grain boundaries shared by the quartz columns may be smooth and gently curved, but are more commonly complexly serrated or stepped. Step offsets coincide with inclusion trails, less often with inclusion bands. The magnitude of the step varies up to 0.75 mm, but is typically 0.2 mm. Across an inclusion trail a stepped quartz grain boundary appears 'displaced' in nearly always the same sense as shear displacement for the vein. Quartz columns with largest steps are inclined at lowest angles to inclusion trails. The steps do not appear to be actual shear displacements of former straight grain boundaries, but are probably formed by the antitaxial quartz fibre growth mechanism described by Cox (1987).

Some slender quartz columns with smooth grain boundaries which are inclined about 60° to the inclusion trails have been later sheared along the boundaries. The displacement of inclusion trails and bands is in the order of 0.1 mm. The orientation and shear sense of these grain boundaries is consistent with them being microshears which are conjugate to the shearing on the bedding plane. Undulose extinction and recrystallization occur in the quartz bordering these sheared boundaries. In the vicinity of some of these recrystallized sheared boundaries the inclusion trails and bands have been 'swept away'. This latter effect was described by Jessell *et al.* (1994) as possibly resulting from primary quartz grain boundary migration. Occasionally inclusion bands may be pulled apart and filled with displacement controlled mica fibres as described by Cox & Etheridge (1983) for intergranular microfractures. These are uncommon but must be carefully distinguished from the original mica fabric defining the inclusion bands.

TYPE II BEDDING-PARALLEL VEINS

Wallrock seams

Well-developed inclusion bands are absent in Type II veins. Type II veins (Fig. 3d) are composed of numerous approximately bedding-parallel quartz bands 0.05–10 mm thick (averaging 1.2 mm). These bands are separated by discontinuous thin seams (0.05–2.0 mm thick, averaging 0.5 mm) of crenulated slate with adherences of wallrock particles giving the seams a lumpy or lenticular appearance. Stylolitization is commonly developed along these wallrock seams.

Traced laterally, some wallrock seams are seen to splay into strands composed of lenses of wallrock (Fig. 7a). In some cases, between the lenses are mica flakes with (001) planes consistently inclined to the seam. Comparison of matching surface irregularities from one wallrock lens to the other indicates that the mica (001)s are aligned parallel to the displacement direction along which these lenses were detached from the seam. They are thus similar to the oriented layer silicate fibres within intragranular microfractures described by Cox & Etheridge (1983).

It is common to find thin wallrock seams incompletely detached from the veinwall or only slightly displaced from it (Fig. 7e). Irregularities in thickness of the partly detached seams are preserved as scalloped irregularities or, more commonly, gentle undulations in the vein margin (Fig. 7e). There are usually complex distortions in the wallrock crenulations associated with these surface irregularities. In some examples minute mica flakes have (001) planes aligned parallel to the extension direction involved in the partial detachment of the wallrock seam. These micas do not have (001) orientations determined by the layer silicates in the veinwall slate, and therefore also appear to be displacement controlled fibres (Cox & Etheridge 1983). In other examples there are inclusion bands developed parallel to the vein wall (Fig. 7d). The extension direction is invariably compatible with the shear sense expected for flexural-slip folding.

Some quartz bands are separated by veinwall-parallel regular thickness ribbons of fine-grained quartz containing minute mica flakes with preferred orientation of (001) planes (Fig. 7f). The (001) planes having the same sense and roughly the same angle of inclination to the ribbon as those micas associated with detached wallrock lenses described above. The fine-grained quartz grains have a preferred *c*-axis orientation parallel to the mica (001) planes. The mica orientations are consistent from ribbon to ribbon in a single vein. The mica (001) planes are interpreted as lying parallel to increments of extensional opening for the vein. The angle of inclination of this extension direction to the vein wall varies from 5° to 77°

(averaging 25°), and the extension direction is invariably compatible with the shear sense expected for flexural-slip folding.

Quartz bands in Type II veins are commonly contaminated by numerous particles of crenulated slate, occasionally giving the veins a mottled appearance in hand specimen (Fig. 7b). The crenulations in the slate particles of the veins are distorted, have highly variable orientation even in adjacent particles (Fig. 7b), and show varying degrees of having been torn apart. Apparently the crenulations in these suspended slate particles formed *before* the particles were disaggregated and incorporated into the vein. The significance of this is discussed further below. The quartz bands of Type II veins are often cluttered by dispersed mica flakes. Some detached wallrock particles in the Type II veins show disintegration into inclusion bands (15–20 μm apart) when the crenulation cleavage trace in the wallrock particle roughly parallels the opening direction for the quartz band enclosing it.

Since nearly all of the examined Type II veins contained contorted crenulated slate fragments it is concluded that most of the veins have formed during or after crenulation development in the host slates. Of course the easiest microstructures to interpret belong to those veins showing the least later deformation. A minority of Type II veins are so deformed that there remains a possibility that such examples may have been deposited earlier.

Type II BPV quartz microstructures

Type II vein quartz is often intensely strained and shows spectacular examples of deformation bands, undulose extinction, mortar texture and mylonitization. Penetrating along seams of intensely deformed quartz are occasional lensoidal veins of coarse-grained weakly or apparently undeformed quartz with simple straight grain boundaries and occasional hexagonal cross-sections. Quartz with extremely variable grainsize is associated with areas of dispersed mica and with veinwall-parallel mica bands. Wallrock fragments are often rimmed in very fine quartz grains, a few grains wide.

DISCUSSION

Development of Type I BPVs

The microstructures of Type I BPVs described above indicate that: (1) the inclusion trails are developed as syntaxial overgrowths upon crenulation cleavage stripes in the vein wall; (2) inclusion bands are developed parallel to the walls of discordant vein segments between these crenulation cleavage stripes; (3) the displacement path for the opening of these veins lies parallel to the inclusion trails, hence involves bedding-parallel shear opening; and (4) the sense of shear related to Type I vein opening is invariably consistent with the shear involved in flexural-slip folding. Both (1) and (2) imply that the formation of Type I vein microstructures occurs either during or after pressure-solution differentiation of the crenulation cleavages in the wallrocks. These veins are therefore either syn- or post-crenulation cleavage (or both).

The syn-crenulation cleavage origin proposed for Type I BPVs requires: (a) the simultaneous development of tension veining and shear structures, which is well established and has been described previously by Beach (1975), Ramsay & Huber (1987) and others; and (b) Synchronous development of tension veins and pressure solution effects, which has also been reported, for example, by Price & Cosgrove (1990) (p. 471). The syn-crenulation cleavage model (as opposed to post-crenulation) is preferred here firstly because it provides a local source of vein mineral components via dissolution of materials during cleavage differentiation. Secondly, precipitation in BPVs of syntaxial vein phyllosilicates on *P*-domains at the vein contact would then be synchronous with recrystallization of phyllosilicates within the crenulation cleavage *P*-domains (Stephens *et al.* 1979, White & Johnston 1981). Finally, it provides a ready mechanism to explain how Type I BPVs may grow in thickness. By this model, the thickness would be expected to increase as bedding-parallel shearing proceeds, due to continuous propagation of existing tension veins or initiation of new tension veins during shearing on vein walls. Whilst the syn-crenulation cleavage model is favoured, it is acknowledged that a post-cleavage origin is also a possibility.

A model for the syn-crenulation cleavage development of Type I BPVs is briefly described below and is illustrated in Figs. 8 & 9. According to this model, the events leading to the formation of Type I BPVs are:

(1) Microfolding of compaction/diagenetic bedding-parallel fabric and pressure-solution differentiation in slates, after significant limb dips were attained (Gray & Willman 1991) producing a crenulation cleavage fabric.

(2) Tensional stresses associated with bedding-parallel shear (perhaps imposed upon the slate beds beneath stronger sandstone beds) generating crenulation- and bedding-discordant tensional veins (Figs. 8a & 9a).

(3) Continued flattening and pressure-solution differentiation of the crenulations producing segmentation and rotation of the tension veins to lower angles of inclination with the BPV wall (Figs. 8a & 9b)

(4) Crack–seal opening of the segmented tension veins in the direction parallel to bedding during (3), so that phyllosilicate grains which have grown syntaxially upon the crenulation cleavage stripes are detached during crack–seal vein opening, leading to the development of bedding-parallel inclusion trails which track the displacement path during vein opening, as in the models described by Ramsay & Huber (1983) and Cox & Etheridge (1983) (Fig. 9c). Either or both syntaxially-grown phyllosilicates and wallrock phyllosilicate particles are detached from the tension vein walls to produce inclusion bands. Chance plucking of wallrock fragments from the vein walls controls the evolving shape of inclusion bands during vein growth (Fig. 9d). The vein

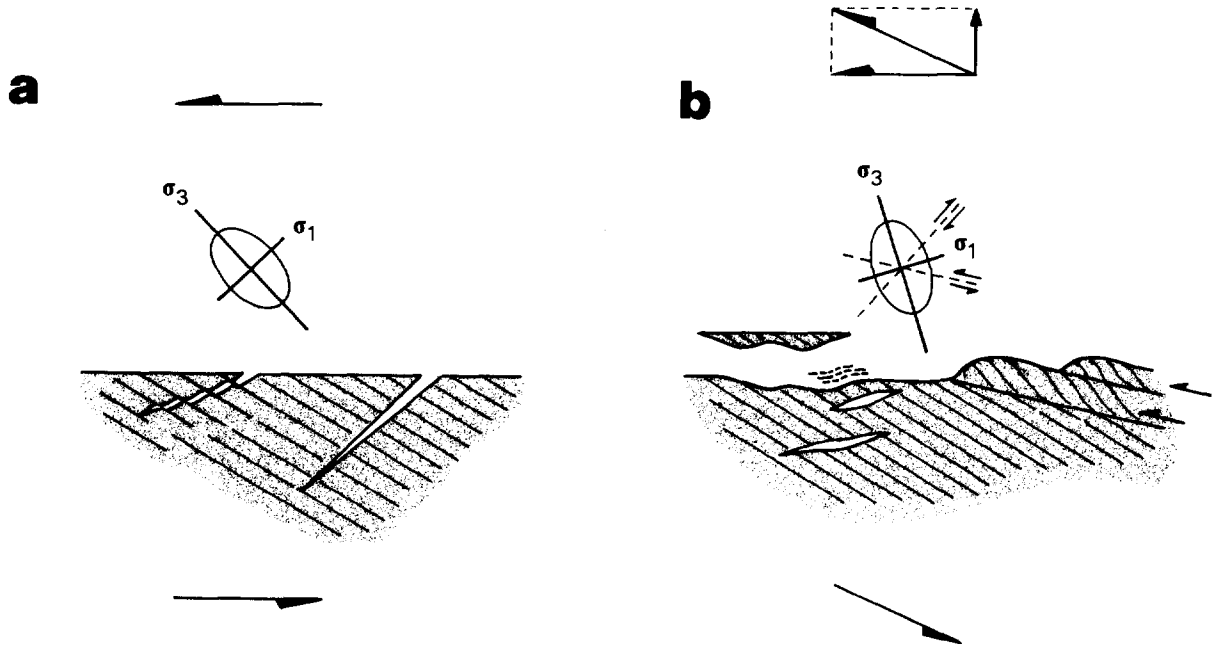

Fig. 8. A model to explain how BPV Types I and II may form as a result of different stress orientations associated with dilation or no dilation normal to beds, respectively, during bedding-parallel shear. In both figures the orientation of bedding is approximately along the vein contact (apart from deformation effects). Crenulation cleavage orientation is represented by oblique lines in the veinwalls. (a) Bedding parallel shear with no dilation component normal to the vein wall, leading to Type I BPVs (see Fig. 9 for the development of Type I veins beyond this stage). This situation yields a minimum principal stress direction σ_3 lying at a low angle to wallrock crenulation cleavage. Discordant tension veins form and are modified by continuing flattening rotation and pressure solution during vein opening leading to vein segments lying at a lower angle to the vein wall. The maximum principal stress direction σ_1 lies not far from normal to the cleavage *P*-domains and may contribute to pressure solution effects. (b) Bedding parallel shear with some dilation component normal to the vein wall leading to Type II BPVs. The minimum principal stress direction σ_3 lies at a large angle to the vein wall and generates tension veins at a low angle to the vein wall. As these tension veins grow they may split off slices of wallrock producing seams. Alternatively inclusion bands or quartz-mica ribbons may result if crack–seal increments are small. The low angle of the maximum principal stress direction σ_1 to the vein wall results in thrusting at the vein wall.

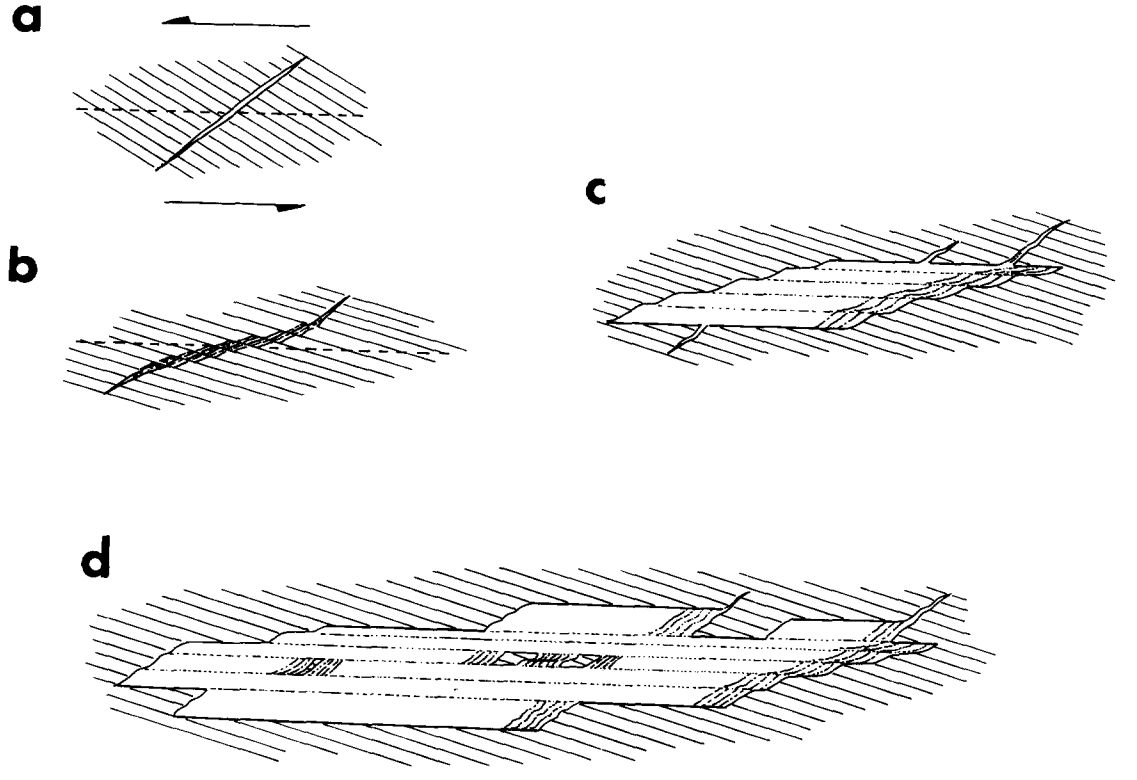

Fig. 9. A sketch showing the stages of development of Type I bedding-parallel veins. The bedding trace is represented by the dashed lines. (a) Initial tension vein forms discordant to bedding and cleavage. (b) Flattening, rotation, and segmentation of veins by pressure solution occurs during crack–seal vein opening. (c) Rhomb-opening of the tension gash segments produces inclusion trails tracking the opening direction (parallel to bedding), and inclusion bands parallel to the discordant vein segments. (d) Continued dilation of the tension veins. Propagation of tension veins into the veinwall and their dilation increases the thickness of the Type I vein. Detached wallrock fragments occupy the centre of the vein.

opening mechanism produces rhomb-shaped veins similar to those described by Gaviglio (1986) and Labaume *et al.* (1991). However, the present model differs in having pressure-solution and other cleavage-related deformation effects modifying the tensional veins during crack–seal opening. Such continuing deformation may account for lower angles of inclination of inclusion bands and narrower inclusion band arrays than noted by the latter workers.

(5) Continuing propagation and initiation of the discordant veins during progressive shearing would increase the vein thickness and may explain the relationship between vein thickness and magnitude of slip along the vein as noted by Tanner (1989).

The direction of opening of the Type I veins is quite consistent with the sense of shear involved in flexural slip folding, and shows the expected change in shear sense across fold hinges. It is therefore considered that these veins have formed *during* flexural-slip folding. The above conclusions differ from those of Jessell *et al.* (1994), which are considered below.

Development of Type II BPVs

Type II vein microstructures are associated with vein opening histories involving a dilation component. The larger vein normal displacements may explain the greater width of Type II veins. If an applied shear couple is not parallel to bedding (Fig. 8b) then the minimum principal stress σ_3 lies at a large angle to the vein wall, resulting in the formation of tensional veins at low angles to the vein wall and the detachment of slices of wallrock from the vein wall to form wallrock lenses and seams (or of phyllosilicate particles to form inclusion bands) (Fig. 8b). The detachment of large numbers of crenulated wallrock fragments which clutter these veins is suggestive of a syn- or post-crenulation cleavage timing of formation.

An obviously possible explanation for the vein normal extension component is high fluid pressure variation (Cosgrove 1993, Jessell *et al.* 1994). High fluid pressures could hydraulically 'jack' vein walls apart. However, as noted by Jessell *et al.* (1994), high fluid pressures may promote a larger *shear* component by reducing the frictional resistance on the shear planes.

Could any of the Bendigo–Castlemaine BPVs be pre-folding?

In the Bendigo–Castlemaine region there is no evidence to suggest that the BPV veining is due to pre-folding fluid overpressures due to fluid accumulation beneath impermeable rocks (Henderson *et al.* 1990). Nearly all of the BPVs in this region lie just beneath permeable sandstones or at their contact with slates. In the post-cleavage model of Mawer (1987), for late syn-folding origin of BPVs, he suggested that silicified sandstones formed an impermeable barrier for fluids. Silicification of sandstones above BPVs is not consistently found in the Bendigo–Castlemaine area. Graves & Zentilli (1982) ascribed fluid overpressures to the greater rates of metamorphic fluid generation (in slates) and supply (from sandstone reservoirs) compared to lateral rates of fluid loss to explain BPVs in slates near sandstones. However, the Bendigo–Castlemaine BPVs are wider spaced (hence fewer) in the pelite-dominated sequences (Jessell *et al.* 1994). Nevertheless, Type II veins are intensely deformed and it is possible that a few of them could have formed before cleavage and folding.

Interestingly Fitches *et al.* (1986) note that the pre-folding BPVs of hydraulic-jacking origin occur mainly in homogeneous argillites or at the *upper* contact of a sandstone bed with overlying argillites. The most favoured sites for flexural-slip related BPVs are at the lower contact of a sandstone bed with the underlying slate (Tanner 1989).

Comparison of the syn-crenulation model with the early-folding model by Jessell et al. (1994)

On the basis of studying the BPVs of the Bendigo–Castlemaine area, Jessell *et al.* (1994) proposed that Type I BPVs formed as follows:

(1) The BPVs occur along those bedding horizons where cyclic pore-fluid pressures jacked apart bedding planes, before folds were initiated.

(2) Reduced friction along bedding planes, as a result of (1), helped locate folds in those areas of high fluid pressure (explaining the association of BPVs with folds).

(3) Incompetent layers (shales) shortened parallel to layering while overlying competent layers (sandstones) began to buckle, leading to length mismatch along protofold limbs.

(4) The above mismatch led to a reverse sense of shear displacement across the BPV walls compared to the shear sense associated with flexural-slip folding.

(5) Phyllosilicate inclusion surface traces (ISTs-equivalent to the inclusion bands and trails of this study) formed by syntaxial growth and detachment of micas on bedding planes (which formed the vein walls) along the line of intersection of early formed cleavages.

(6) The parallelism to bedding of mica (001)s in the ISTs (acknowledged as a problem for this model) were suggested to have been rotated away from normal to the shortening direction in an early stage of layer parallel slip, before being incorporated into the ISTs.

(7) The ramps (here inclusion bands) and flats (here inclusion trails) of the ISTs represent relatively large and small veinwall-parallel shear, respectively, compared to vein dilation. The relative contributions of shear and dilation were controlled by fluid pressure through its effects on shear resistance.

Jessell *et al.* (1994) considered four possible models to explain the ISTs. Two models were quickly eliminated (pressure solution or shear truncation of ramp ISTs) on the basis of the continuity of elongate quartz grains across the ISTs. The remaining two models included that of Ramsay & Huber (1983), and their favoured model (summarised above). Ramsay and Huber's (1983) model

interprets ramp and flat ISTs as reflecting steplike (*en échelon*) irregularities in the vein wall with the vein opening direction approximately parallel to the flats (that is, approximately parallel to the veinwall). This was the model preferred by Gaviglio (1986) and Labaume *et al.* (1991) to explain steplike inclusion surfaces in veins associated with dilatant shearing. Jessell *et al.*'s objections to applying Ramsay and Huber's (1983) model to the Bendigo–Castlemaine BPVs were that:

(1) The flat ISTs (here inclusion trails) were not like the 'transform' structures described by Labaume *et al.* (1991) which separate matrix bands formed by repeated plucking of wallrock particles at veinwall releasing oversteps.

(2) Wallrock particles adhered only to the flat ISTs not the ramps (here inclusion bands).

(3) The BPV veinwalls are planar bedding surfaces not *en échelon* fractures.

(4) Curvature of ISTs in sections parallel to bedding or perpendicular to the lineation, compared to the nearly rectilinear IST traces in sections normal to bedding (and parallel to the slip lineation) requires an odd geometry of fracturing.

(5) Shearing parallel to veinwalls offers no mechanism for creating space to allow vein growth.

(6) The ramp ISTs were much lower angle (20°) than the steeper inclined inclusion bands (50–60°) described by Gaviglio (1986) and Labaume *et al.* (1991) and a mechanism for producing such low angle fractures was difficult to imagine.

However, on the basis of the present study, the model proposed by Ramsay & Huber (1983) appears to best describe the evolution of Type I vein microstructures in the Bendigo–Castlemaine region. It is necessary therefore to consider each of the objections of Jessell *et al.* (1994) to this model. The following are comments regarding each objections listed above.

(1) 'Transform' (shear band) structures such as those described by Labaume *et al.* (1991) do occur in the Bendigo–Castlemaine BPVs and are illustrated in Figs. 4(a) & 5 (a) and (b).

(2) Crenulated wallrock particles do adhere to the ramp ISTs (inclusion bands) as shown in Figs. 5 (a–c).

(3) The BPV walls are occasionally stepped as shown in Fig. 5(d).

(4) The three-dimensional surface geometry of the inclusion trails is controlled in the plane normal to bedding (and parallel to the slip lineation) by the direction of vein opening and in other planes by the geometry of the tension fractures forming the walls of the discordant veins. Neither is an unusual geometry.

(5) The mechanism of Type I vein growth has been described above.

(6) The low angles of the ramp ISTs (inclusion bands) are due to rotation of the discordant tension vein segments during continued flattening, associated with cleavage development.

There are several problems associated with the model of Jessell *et al.* (1994) for the development of Type I BPV structures. These are listed below:

(1) For reversals of apparent shear sense in the Type I veins to routinely occur across fold hinges, the future fold hinges must normally be set in their final locations before limb dips reach a degree or two. This is very unlikely since at such low limb dips 'hinge zones' are very broad and gently rounded and most likely to experience significant hinge mobility. They acknowledge that later hinges are not necessarily even parallel to the early ones in their discussion of the fold at Little Bendigo where the lineations are folded around a synclinal hinge.

(2) Type I veins apparently cease to form without clear reason after the early stages of layer shortening despite the factors involved in their formation (shear parallel to vein walls combined, in their model, with fluid pressure assisted dilation normal to the vein walls) continuing to operate during flexural-slip folding (Cosgrove 1993). Instead the flexural-slip process is suggested to develop only Type II veins (which also involve shearing and dilation).

(3) The (001) planes of the phyllosilicates in the inclusion bands generally do not have constant orientation within each band as they have suggested. The inclined inclusion bands have wallrock ornaments, and the bands change their shape details in accord with fragmentation of these wallrock ornaments in the direction parallel to the vein wall. These bands therefore are not inclusion trails and do not track the displacement path involved in vein opening.

(4) Type I structures are also found in BPVs entirely within siltstones hence the presence of a nearby overlying sandstone is not necessary for their formation.

Inclusion band spacing in the Type I BPVs and flexural-slip increments

The measured spacing of inclusion bands in the direction of opening of a Type I BPV is highly variable even along individual laminae, and rather large for crack–seal increments. The size of these opening increments may explain the absence of inclusion trails which cut through the inclusion bands (such as those described by Cox 1987), and the absence of fibre structures parallel to the direction of vein opening.

The average inclusion band spacing may be an indication of the average magnitude of discrete slip increments involved in a stick–slip model of flexural-slip folding. There is no reason to believe that every opening increment will successfully leave a band of detached phyllosilicate particles from the wallrock steps, so the 0.5 mm average value may be regarded as a maximum average value of the net slip increments. A similar conclusion regarding the relations between crack–seal and stick–slip shear behaviour was reached by Gaviglio (1986). The variability of these increments along a lamina may be related to the lubricative effects of fluid such as the stick–slip behaviour during folding suggested by Cosgrove (1993), or to sporadic hinge migration jamming during evolution of boxfolds to chevron discussed by Fowler & Winsor (1996).

CONCLUSIONS

In the Bendigo–Castlemaine goldfields, bedding-parallel veins (BPVs) are commonly encountered on the limbs of chevron folds. They are almost always located in slate beds, typically within 10 cm of their contact with an overlying sandstone bed. The BPV spacing is irregular but they have an average stratigraphic spacing of about 9 m. BPVs are continuous along dip and strike directions, and the thicker examples are commonly traceable across fold hinges. The thinner examples are in the majority and are generally not traceable over fold hinges. The division of BPVs into microstructural Type I and II veins (Willman 1988, Jessell *et al.* 1994) for this region is confirmed. Individual BPVs may contain both microstructural types.

Type I BPVs contain phyllosilicate inclusion trails subparallel to bedding. These trails track the opening direction of the veins (which therefore involves bedding-parallel shear) and have formed by detachment of syntaxially grown phyllosilicates from prominent crenulation cleavage stripes in the slate vein wall. (The crenulation cleavage is a first generation axial planar structure overprinting a probably compaction-related bedding-parallel fabric.) The inclusion trails enclose systematically inclined inclusion bands formed by a crack–seal process of detachment of phyllosilicates from the walls of dilating discordant tension veins, which have been segmented by pressure-solution processes associated with crenulation cleavage formation, and have been rotated to lower angles during continued cleavage-related flattening. The discordant tension vein segments have a rhomb-opening mechanism similar to that described by Gaviglio (1986) and Labaume *et al.* (1991). Type I veins have formed during and/or after crenulation cleavage development in the slaty wallrocks, and show a shear sense of opening invariably consistent with that involved in flexural-slip folding. Type I veins grow in thickness by opening and propagation of the discordant tension veins into the BPV wall. The ramp ISTs described by Jessell *et al.* (1994) are not inclusion trails tracking the opening history of the veins. The vein opening mechanism is similar to that described by Ramsay & Huber (1983) and also concluded by Cox (1987) for the laminated portions of a BPV from Castlemaine.

Type II veins involve a vein-normal opening component and consist of quartz bands separated by stylolitized wallrock seams. These veins generally contain torn-apart fragments of crenulated slate and therefore also appear to postdate the onset of crenulation cleavage development in these rocks. The sense of shear involved in the opening of Type II BPVs is also invariably consistent with that required by flexural-slip folding. On the basis of these microstructures it is considered that both Type I and II BPVs have formed essentially during flexural-slip folding. However, the existence of some intensely deformed Type II veins with indecipherable primary textures does not preclude the possibility that a minority of the veins may be pre-folding.

Inclusion band spacing in the Type I veins probably represents slip increments averaging 0.5 mm during flexural-slip folding. The variability of these increments is consistent with proposals of Cosgrove (1993) on stick–slip flexural-slip folding activity.

Acknowledgements—The author would like to thank Dianne Aulsebrook for preparation of vein thin sections, and to acknowledge the helpful suggestions of two anonymous referees which improved the presentation of this paper.

REFERENCES

Barnett, D. E. & Chamberlain, C. P. 1988. Structurally controlled fluid migration during folding and regional metamorphism, east Vermont, U.S.A. *Geol. Soc. Am. Abstr. Prog.* **20**, A45–A46.

Beach, A. 1975. The geometry of en-échelon vein arrays. *Tectonophysics* **28**, 245–263.

Boulter, C. A. 1979. On the production of two inclined cleavages during a single folding event; Stirling Range, S. W. Australia. *J. Struct. Geol.* **1**, 207–219.

Boyle, R. W. 1986. Gold deposits in turbidite sequences: their geology, geochemistry and history of the theories of their origin. In: *Turbidite-hosted Gold Deposits* (edited by Keppie, J. D., Boyle, R. W. & Haynes, S. J.). *Spec. Pap. geol. Assoc. Can.* **32**, 1–13.

Chace, F. M. 1949. Origin of the Bendigo saddle reefs with comments on the formation of ribbon quartz. *Econ. Geol.* **44**, 561–597.

Cosgrove, J. W. 1993. The interplay between fluids, folds and thrusts during the deformation of a sedimentary succession. *J. Struct. Geol.* **15**, 491–500.

Cosgrove, J. W. 1995. The interplay between fluids, folds and thrusts during the deformation of a sedimentary succession: Reply. *J. Struct. Geol.* **17**, 1479–1480.

Cox, S. F. 1987. Antitaxial crack-seal vein microstructures and their relationship to displacement paths. *J. Struct. Geol.* **9**, 779–787.

Cox, S. F. & Etheridge, M. A. 1983. Crack–seal fibre growth mechanisms and their significance in the development of oriented layer silicate microstructures. *Tectonophysics* **92**, 147–170.

Cox, S. F., Etheridge, M. A., Cas, R. A. F. & Clifford, B. A. 1991. Deformational style of the Castlemaine area, Bendigo–Ballarat Zone: Implications for evolution of crustal structure in central Victoria. *Aust. J. Earth Sci.* **38**, 151–170.

Fitches, W. R., Cave, R., Craig, J. & Maltman, A. J. 1986. Early veins as evidence of detachment in the Lower Palaeozoic rocks of the Welsh Basin. *J. Struct. Geol.* **8**, 607–620.

Fitches, W. R., Cave, R., Craig, J. & Maltman, A. J. 1990. The flexural-slip mechanism: Discussion. *J. Struct. Geol.* **12**, 1081–1083.

Fowler, T. J. & Winsor, C. N. 1996. Evolution of chevron folds by profile shape changes: comparison between multilayer deformation experiments and folds of the Bendigo–Castlemaine goldfields, Australia. *Tectonophysics* **258**, 125–150.

Gaviglio, P. 1986. Crack–seal mechanism in a limestone: a factor of deformation in strike-slip faulting. *Tectonophysics* **131**, 247–255.

Graves, M. C. & Zentilli, M. 1982. A review of the geology of gold in Nova Scotia. In: *Geology of Canadian Gold Deposits Canad. Inst. Min. Metall. Spec. Pap.* **24**, 233–242.

Gray, D. R. 1979. Microstructure of crenulation cleavages: an indicator of cleavage origin. *Am. J. Sci.* **279**, 97–128.

Gray, D. R. 1988. Structure and Tectonics. Bendigo–Ballarat Zone. In: *Geology of Victoria* (edited by Douglas, J. G. & Ferguson, J. A.). *Geol. Soc. Aust. Inc.*, Melbourne, 10–11.

Gray, D. R. & Willman, C. E. 1991. Thrust-related strain gradients and thrusting mechanisms in a chevron-folded sequence, southeastern Australia. *J. Struct. Geol.* **13**, 691–710.

Haynes, S. J. 1987. Classification of quartz veins in turbidite-hosted gold deposits, greenschist facies, eastern Nova Scotia. *Can. Instit. Min. Metall. Trans.* **80**, 37–51.

Henderson, J. R., Wright, T. O. & Henderson, M. N. 1986. A history of cleavage and folding: an example from the Goldenville Formation, Nova Scotia. *Geol. soc. Am. Bull.* **97**, 1354–1366.

Henderson, J. R., Wright, T. O. & Henderson, M. N. 1989. Mechanics of formation of gold-bearing quartz veins, Nova Scotia, Canada—Comment. *Tectonophysics* **166**, 351–352.

Henderson, J. R., Henderson, M. N. & Wright, T. O. 1990. Water-sill hypothesis for the origin of certain veins in the Meguma Group, Nova Scotia, Canada. *Geology* **18**, 654–657.

Jessell, M. W., Willman, C. E. & Gray, D. R. 1994. Bedding parallel veins and their relationship to folding. *J. Struct. Geol.* **16**, 753–767.

Keppie, J. D. 1976. Structural model for the saddle reef and associated gold veins in the Meguma Group, Nova Scotia. *Can. Inst. Min. Metall. Trans.* **69**, 103–116.

Labaume, P., Berty, C. & Laurent, Ph. 1991. Syn-diagenetic evolution of shear structures in superficial nappes: an example from the Northern Apennines (NW Italy). *J. Struct. Geol.* **13**, 385–398.

Mawer, C. K. 1987. Mechanics of formation of gold-bearing quartz veins, Nova Scotia, Canada. *Tectonophysics* **135**, 99–119.

Mawer, C. K. 1989. Mechanics of formation of gold-bearing quartz veins, Nova Scotia, Canada—Reply. *Tectonophysics* **166**, 352–354.

McKinstry, H. E. & Ohle, E. L. 1949. Ribbon structure in gold quartz veins. *Econ. Geol.* **44**, 87–109.

Nicholson, R. 1978. Folding and pressure solution in a laminated calcite–quartz vein from the Silurian slates of the Llangollen region of N Wales. *Geol. Mag.* **115**, 47–54.

Price, N. J. & Cosgrove, J. W. 1990. *Analysis of Geological Structures*. Cambridge University Press, Cambridge.

Ramsay, J. G. 1967. *Folding and Fracturing of Rocks*. McGraw-Hill, New York.

Ramsay, J. G. 1980. The crack–seal mechanism of rock deformation. *Nature* **284**, 135–139.

Ramsay, J. G. & Huber, M. I. 1983. *The Techniques of Modern Structural Geology*. Vol. 1. Academic Press Inc., London.

Ramsay, J. G. & Huber, M. I. 1987. *The Techniques of Modern Structural Geology*. Vol. 2. Academic Press Inc., London.

Ramsay, W. R. H. & Willman, C. E. 1988. Economic Geology: Gold. In: *Geology of Victoria* (edited by Douglas, J. G. & Ferguson, J. A.). *Geol. Soc. Aust. Inc.*, Melbourne, 454–482.

Smith, J. V. & Marshall, B. 1993. Implications of discrete strain compatibility in multilayer folding. *Tectonophysics* **222**, 107–117.

Stephens, M. B., Glasson, M. J. & Keays, R. R. 1979. Structural and chemical aspects of metamorphic layering development in metasediments from Clunes, Australia. *Am. J. Sci.* **279**, 129–160.

Stone, J. B. 1937. The structural environment of the Bendigo Goldfield. *Econ. Geol.* **32**, 867–895.

Stoneley, R. 1983. Fibrous calcite veins, overpressures, and primary oil migration. *Bull. Am. Ass. Petrol. Geol.* **67**, 1427–1428.

Tanner, P. W. G. 1989. The flexural-slip mechanism. *J. Struct. Geol.* **11**, 635–655.

Tanner, P. W. G. 1990. The flexural-slip mechanism: Reply. *J. Struct. Geol.* **12**, 1084–1087.

Thomas, D. E. 1953. The Bendigo Goldfield. In: *Geology of Australian Ore Deposits* (edited by Edwards, A. B.). Fifth Empire Mining and Metallurgical Congress, Aus. I. M. M., 1011–1027.

van der Pluijm, B. A. 1984. An unusual 'crack-seal' vein geometry. *J. Struct. Geol.* **6**, 593–597.

White, S. H. & Johnston, D. C. 1981. A microstructural and microchemical study of cleavage lamellae in a slate. *J. Struct. Geol.* **3**, 279–290.

Willman, C. E. 1988. Geological Report: Spring Gully 1:10,000 map area, Bendigo goldfield. *Vict. geol. Surv. Rep.* **85**.

Willman, C. E. & Wilkinson, H. E. 1992. Bendigo Goldfield. *Vict. Geol. Surv. Rep.* **93**.

Yang, X. & Gray, D. R. 1994. Strain, cleavage and microstructure variations in sandstone: implications for stiff layer behaviour in chevron folding. *J. Struct. Geol.* **16**, 1353–1365.